THE JOURNAL OF BIOLOGICAL CHEMISTRY VOL. 282, NO. 17, pp. 12725–12733, April 27, 2007

Perturbation of Endoplasmic Reticulum Homeostasis Facilitates Prion Replication*

Received for publication, December 29, 2006, and in revised form, February 27, 2007 Published, JBC Papers in Press, February 28, 2007, DOI 10.1074/jbc.M611909200

Claudio Hetz[‡§1], **Joaquín Castilla**[‡], **and Claudio Soto**[‡2]

From the [‡]*Department of Neurology, University of Texas Medical Branch, Galveston, Texas 77555 and the* [§]*Institute of Biomedical Science, Fondo de Areas Prioritarias Center for Molecular Studies of the Cell, University of Chile, Independencia 1027, P. O. Box 70086, Santiago, Chile*

Prion diseases are fatal and infectious neurodegenerative disorders characterized by the accumulation of an abnormally folded form of the prion protein (PrP), termed PrP^{Sc}. Prion replication triggers endoplasmic reticulum (ER) stress, neuronal dysfunction, and apoptosis. In this study we analyze the effect of perturbations in ER homeostasis on PrP biochemical properties and prion replication. ER stress led to the generation of a misfolded PrP isoform, which is detergent-insoluble and protease-sensitive. To understand the mechanism by which ER stress generates PrP misfolding, we assessed the contribution of different signaling pathways implicated in the unfolded protein response. Expression of a dominant negative form of IRE1α or XBP-1 significantly increased PrP aggregation, whereas overexpression of ATF4 or an active mutant form of XBP-1 and ATF6 had the opposite affect. Analysis of prion replication *in vitro* revealed that the PrP isoform generated after ER stress is more efficiently converted into PrP^{Sc} compared with the protein extracted from untreated cells. These findings indicate that ER-damaged cells might be more susceptible to prion replication. Because PrP^{Sc} induces ER stress, our data point to a vicious cycle accelerating prion replication, which may explain the rapid progression of the disease.

Transmissible spongiform encephalopathies (TSEs),[3] also known as prion-related disorders, are a group of diseases that affects humans and animals and presents a long incubation period, but a rapid clinical progression once symptoms appear. TSEs are characterized by neurological dysfunction that may include dementia, ataxia, and psychiatric disturbances. The central molecular event in the pathogenesis of prion diseases is the conversion of the normal cellular prion protein, termed PrP^{C}, into the pathological form denoted PrP^{Sc} (1). The generation of PrP^{Sc} is associated with defined structural changes, leading to characteristic alterations in the biochemical properties of the protein such as insolubility in non-denaturating detergents and partial resistance to proteases. Although the detailed mechanism of prion conversion is not entirely clear, it involves the formation of conformational intermediates and oligomerization processes (1).

PrP^{C} is a glycosylphosphatidylinositol-anchored protein located in membrane subdomains, denominated detergent-resistant membranes, or lipid rafts (2–4). PrP undergoes a series of post-translational modifications during its passage through the ER, including the addition of the glycosylphosphatidylinositol anchor, the formation of the intramolecular disulfide bond, the removal of the amino- and carboxyl-terminal signal peptides and the initial addition of glycosylation chains (3, 5). Glycosylation is completed in the Golgi apparatus, and the mature protein traffics to the cell surface.

Several pieces of evidence have suggested an important role for cellular PrP trafficking and clearance pathways in PrP^{Sc} formation. Recent studies suggested that malfunction of the protein quality control has an active role in PrP misfolding and neuronal death (reviewed in Ref. 6). Approximately 10% of nascent PrP molecules are subjected to ER-associated degradation (ERAD) through the proteasome (7, 8). ER chaperones, like Grp78/BiP, have been implicated in the process of recognition of misfolded PrP for proteasomal degradation, playing a role in the maintenance of PrP quality control (9). Some PrP mutants associated with hereditary forms of TSEs are accumulated at the ER/Golgi (10–16). Inhibition of the proteasome in cells overexpressing PrP^{C} leads to the cytosolic accumulation of PrP forms that exhibit some of the biochemical properties of PrP^{Sc}, such as insolubility in non-ionic detergents and partial resistance to protease degradation (8, 17, 18). However, this PrP form is not associated with infectivity. The role for the proteasome in PrP^{Sc} formation has also been supported by experiments showing that mild proteasome inhibition leads to apoptosis only in cells chronically infected with scrapie prions and not in control cells (19). This toxic effect is associated with the formation of

* This work was supported by National Institutes of Health Grants NS049173 and NS050349 (to C. S.), the Fondo Nacional de Ciencia y Desarrollo (FONDECYT) (Grant 1070444 to C. H.), the Fondo de Areas Prioritarias (FONDAP) (Grant 15010006 to C. H.), and a Post Doctoral Fellowship from Damon Runyon Cancer Research Foundation (to C. H.). The costs of publication of this article were defrayed in part by the payment of page charges. This article must therefore be hereby marked "*advertisement*" in accordance with 18 U.S.C. Section 1734 solely to indicate this fact.

[1] To whom correspondence may be addressed: Program of Cellular and Molecular Biology, Inst. of Biomedical Sciences (ICBM), Faculty of Medicine, University of Chile, Independencia 1027, P. O. Box 70086, Santiago, Chile. Tel.: 56-2-9786849; Fax: 56-2-9786871; E-mail: chetz@med.uchile.cl.

[2] To whom correspondence may be addressed: Dept. of Neurology, University of Texas Medical Branch, 301 University Boulevard, Galveston, TX 77555. Tel.: 409-747-0017; Fax: 409-747-0020; E-mail: clsoto@utmb.edu.

[3] The abbreviations used are: TSE, Transmissible spongiform encephalopathy; ATF6, activating transcription factor 6; BCA, bicinchoninic acid; ER, endoplasmic reticulum; ERAD, ER-associated degradation; FCS, fetal calf serum; GFP, green fluorescent protein; Grp, glucose-regulated proteins; IRE1α, inositol-requiring transmembrane kinase and endonuclease; MTS, 3-(4,5-dimethylthazol-2-yl)-5–3-carboxymethoxyphenyl)-2-(4-sulfophenyl)-2H-tetrazolium; PERK, double-stranded RNA-activated protein kinase-like ER kinase; PMCA, protein-misfolding cyclic amplification; PK, proteinase K; PrP, prion protein; UPR, unfolded protein response; XBP-1, X-Box binding protein-1.

intracellular protein aggregates in aggresomes containing PrP^{Sc}, chaperones, ubiquitin, and proteasome subunits (19).

Alteration of ER homeostasis leads to the accumulation of misfolded proteins in this organelle activating the unfolded protein response (UPR) (20, 21). Activation of the UPR triggers the up-regulation of multiple chaperones, folding enzymes, and proteins involved in the ERAD pathway (20). In this way, the UPR increases the folding capacity of the ER and reduces the load of unfolded proteins (20). The UPR is controlled by the activation of three stress sensors located on the ER membrane, known as IRE1α (inositol-requiring transmembrane kinase and endonuclease), PERK (double-stranded RNA-activated protein kinase-like ER kinase), and ATF6 (activating transcription factor 6). IRE1α is a Ser/Thr protein kinase/endoribonuclease that, upon activation, initiates the unconventional splicing of the mRNA encoding the transcriptional factor X-Box-binding protein 1 (XBP-1) (22, 23). This leads to the formation of a more stable and potent transcriptional activator. Spliced XBP-1 up-regulates a subset of UPR-related genes involved in protein folding and ERAD (24). PERK directly phosphorylates and inhibits the translation initiation factor eIF2α, decreasing the overload of misfolded proteins in the ER (20). Conversely, eIF2α phosphorylation activates the translation of the activating transcription factor 4 (ATF4), which also induces UPR-related genes. A third UPR pathway is initiated by ATF6, a type II ER transmembrane protein, encoding a bZIP transcriptional factor on its cytosolic domain (25). Upon ER stress, ATF6 is exported to the Golgi, where it is processed. Cleaved ATF6 then translocates to the nucleus where it increases the expression of *grp78/bip* and *xbp-1* transcription (23).

When the stress level overcomes the ability of the cell to control the overload of misfolded proteins in the ER, specific pro-apoptotic components trigger cellular death. This pathway is not well characterized yet and includes the induction of the transcriptional factor CHOP/GADD153 (26, 27), up-regulation of pro-apoptotic members of the BCL-2 protein family (28), and activation of several caspases, including the ER-resident caspase-12 in rodents (29–31). We and others have previously shown that ER stress plays an important role on TSE pathogenesis (32–38). The up-regulation of UPR-responsive chaperones, such as Grp78/BiP, Grp94, and Grp58, was observed in the cortex of patients affected with variant and sporadic Creutzfeldt-Jakob disease (33, 38), in mice infected with scrapie prions, and in neuroblastoma cells treated with brain-derived PrP^{Sc}. Moreover, overexpression of the disulfide isomerase Grp58 was shown to be an early event in prion pathogenesis, closely following PrP^{Sc} formation (37). The interaction between PrP and this chaperone modulates the neurotoxic activity of PrP^{Sc} (37).

In this study we explored the involvement of ER stress in prion replication. Our results indicate that treatment of Neuro2A cells or primary cortical neurons with different compounds that specifically alter ER homeostasis led to the formation of detergent-insoluble misfolded PrP aggregates. No significant changes on total PrP levels or on the targeting of PrP to the plasma membrane were observed. Mechanistically, we showed that expression of spliced XBP-1, ATF6, or ATF4 decreased accumulation of misfolded PrP aggregates under ER stress conditions, whereas expression of a dominant negative form of IRE1α and XBP-1 increased PrP aggregation. Using the protein misfolding cyclic amplification (PMCA) assay (39) to produce the cell-free conversion of PrP^{C} into PrP^{Sc}, we demonstrated that a PrP substrate from cells subjected to ER stress is more rapidly and efficiently converted into PrP^{Sc} than the protein from healthy cells. Our results suggest that alterations of ER homeostasis may influence the folding of PrP, forming an intermediate more prone to form PrP^{Sc}. These findings have important implications for understanding the molecular basis of prion replication and to develop novel strategies for treatment.

MATERIALS AND METHODS

Cell Culture, Viability Assay, and Transfections—Neuro2A cells were cultured in Dulbecco's modified Eagle's medium supplemented with 10% fetal calf serum and antibiotics (10,000 units/ml penicillin and 10 μg/ml streptomycin), at 37 °C and 5% CO_2. Cell viability was quantified using 3-(4,5-dimethylthazol-2-yl)-5,3-carboxymethoxyphenyl)-2-(4-sulfophenyl)-2H-tetrazolium (MTS) and phenazine methosulfate (CellTiter96® Aqueous, Promega, Madison, WI) assays.

Expression vector for green fluorescent protein (GFPu) construct was kindly provided by R. Kopito (Stanford University, Stanford, CA) (40). Murine PrP was cloned by reverse transcription-PCR from Neuro2A RNA and cloned into pCDNA3 using the HindIII and EcoRI restriction sites. Mouse PrP with the hamster epitope 3F4 was designed as previously described (41). Green fluorescent protein (GFP) was fused to the amino-terminal of PrP at codon 25. Stably expressing Neuro2A cells were produced by transfection using SuperFect kit (Qiagen, Valencia, CA) following the manufacturer's instructions as described before (37). The production of expression vectors for HA-IRE1α, HA-IRE1$\alpha\Delta$C (42), XBP-1s, XBP-1DN (24, 43), ATF6ΔC (25), ATF4, and MYC-CHOP (27) was previously described.

PrP Analysis—To assess detergent insolubility, post-nuclear cell lysates were generated in 1.5% Nonidet P-40 prepared in phosphate-buffered saline in the presence of protease inhibitors (Roche Applied Science). Cell lysates were diluted in 5% Sarkosyl and centrifuged in a TL100 centrifuge at 48,000 rpm for 1 h at 4 °C, and pellets were analyzed by Western blot. Alternatively, before harvesting the cells, a treatment with 5 units/ml phosphatidylinositol-phospholipase C was performed. Protease resistance was assessed by treating post-nuclear extracts with proteinase K (PK, 5 or 50 μg/ml) for 30 min at 37 °C, and the reaction was stopped by adding phenylmethylsulfonyl fluoride followed by boiling in electrophoresis sample buffer. PrP was analyzed by Western blot. PrP immunofluorescence was performed as described before (38).

SDS-PAGE and Western Blot Analysis—Cell lysates were prepared in radioimmune precipitation assay buffer (20 mM Tris, pH 8.0, 150 mM NaCl, 0.1% SDS, 0.5% deoxycholic acid detergent, 0.5% Triton X-100) containing a protease inhibitor mixture (Roche Applied Science). Protein concentration was determined by micro-BCA assay (Pierce). The equivalent of 30–50 μg of total protein was loaded onto 4–12% SDS-PAGE minigels (Novex NuPage, Invitrogen) and analyzed by Western

blotting as described before (37). The following antibodies and dilutions were used: 6H4 anti-PrP 1:10,000 (Prionics, Zurich, Switzerland), 3F4 anti-PrP 1:10,000 (Signed Laboratories), anti-Caspase-12, 1:5,000 (Exalpha, Watertown, MA), anti-Grp78/Bip and anti-Grp58, 1:5,000 (StressGene, San Diego, CA), anti-HA, 1:1,000 (Roche Applied Science), anti-Myc, 1:2,000 (Santa Cruz Biotechnology, Santa Cruz, CA), anti-XBP-1, 1:1,000 (kindly provided by Laurie Glimcher), ATF4, 1,1000 (Santa Cruz Biotechnology), and ATF6, 1:1,000 (kindly provided by Laurie Glimcher). pCDNA-dn-XBP was constructed by removing the region downstream of the EcoRV site of XBP-1s cDNA in the pCDNA-XBP-1s plasmid. For the generation of IRE1α constructs, PCR-amplified human IRE1α cDNA was ligated with a linker containing the HA tag sequences, and then inserted into pMSCVhygro plasmid (Clontech, Mountain View, CA) between BglII and XhoI sites to generate IRE1α-HA. IRE1α-(N)-HA containing the amino acid sequences of 1–500 of human Ire1α was constructed by inserting the PCR-amplified fragment of IRE1α cDNA (5′-GGAGATCTCGCCATGC-CGGCCCGGCGG-3′ and 5′-GGACGCGTGGGTGGAAGG-GCAGCTGC-3′, restriction enzyme sites are underlined) into the vector, which had HA tag sequences.

RNA Extraction and Reverse Transcription-PCR—Total RNA was prepared from primary cortical neurons using TRIzol (Invitrogen), and cDNA was synthesized with SuperScript III (Invitrogen) using random primers $p(dN)_6$ (Roche Applied Science). Quantitative real-time PCR reactions employing SYBR green fluorescent reagent were done in an ABI PRISM 7700 system (Applied Biosystems, Foster City, CA). The relative amounts of mRNAs were calculated from the values of comparative threshold cycle by using β-actin as control. Primer sequences were designed by Primer Express software (Applied Biosystems). Real-time PCR was performed as previously described (44) using the following primers: *grp78/bip*, 5′-TCA-TCGGACGCACTTGGAA-3′ and 5′-CAACCACCTTGAAT-GGCAAGA-3′; *grp58*, 5′-GAGGCTTGCCCCTGAGT-ATG-3′ and 5′-GTTGGCAGTGCAATCCACC-3′; *Chop/gadd153*, 5′-GTCCCTAGCTTGGCTGACAGA-3′ and 5′-TGGAGAGCGAGGGCTTTG-3′; and *xbp-1*, 5′-CCTGAGCC-CGGAGGAGAA-3′ and 5′-CTCGAGCAGTCTGCGCTG-3′.

XBP-1 mRNA splicing assay was done as previously described (43, 45). In brief, PCR primers 5′-ACACGCTTGGG-AATGGACAC-3′ and 5′-CCATGGGAAGATGTTCTGGG-3′ encompassing the spliced sequences in *xbp-1* mRNA was used for the PCR amplification with AmpliTaq Gold polymerase (Applied Biosystems). We separated the PCR products by electrophoresis on a 3% agarose gel (Agarose-1000, Invitrogen) and visualized them by ethidium bromide staining.

Primary Cortical Neurons—Cortical neurons were prepared from mouse embryos at E16.5. Pregnant mice were killed by CO_2 exposure, and embryos were removed under sterile conditions. Brain cortexes were collected, meninges were eliminated, and the tissue was treated with trypsin for 15 min at 37 °C. The cells were then dissociated by two successive trituration and sedimentation steps. Cells were resuspended in Dulbecco's modified Eagle's medium containing 10% horse serum and plated at a density of 1.6×10^6cells/well on polylysine precoated 6-well plates (BD Bioscience). After 4 h of culture, medium was changed by neurobasal medium supplemented with B27 (1×), 2 mM glutamine, penicillin (100 units/ml), and streptomycin (100 g/ml). After 3 days of culture, 4 μM Ara-C was added for 48 h to prevent the proliferation of non-neuronal cells. After 2 days of recovery, cells were subjected to the experiments.

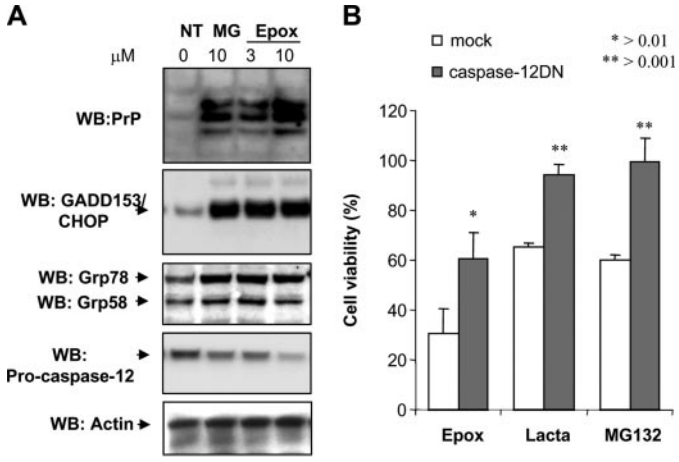

FIGURE 1. **Proteasome inhibitors induce ER stress in Neuro2A cells.** *A*, N2A-mPrP cells were treated with 15 μM MG132 (*MG*) or 6 μM epoxomycin (*Epox*) for 16 h, and the levels of PrP, GADD153/CHOP, Grp58, Grp78/Bip, and pro-caspase-12 were determined by Western blot. *B*, Neuro2A cells stably transfected with a dominant negative form of caspase-12 (*caspase-12DN*) or empty vector (*mock*) were treated with 6 μM epoxomycin (*Epox*), 15 μM lactacystin (*Lacta*), or 15 μM MG132, and after 24 h of incubation cell viability was determined by the MTS assay. Data show the mean ± S.D. of two different experiments performed in triplicate. *NT*, non-treated cells.

Protein Misfolding Cyclic Amplification—Neuro2A cells stably transfected with PrP-3F4 were treated with 6 μM epoxomycin or 50 μM brefeldin A for 16 h. Post-nuclear extracts were generated in phosphate-buffered saline containing 1% Triton X-100 and 1.5% Nonidet P-40. Cell lysates were mixed with different dilutions of brain homogenates (10% prepared in phosphate-buffered saline) from mice infected with the Rocky Mountain Laboratory scrapie strain. Eight PMCA cycles were performed, each consisting of 4-h incubation and one sonication step (10 pulses with 10% power) using a manual sonicator (Bandelin Electronic, model Sonopuls, Germany). As controls, identical samples were frozen at −70 °C without amplification. After PMCA, samples were treated with 50 μg/ml PK for 1 h at 45 °C and analyzed by Western blot using 3F4 anti-PrP antibody.

RESULTS

Proteasome Inhibition Triggers ER Stress—Inhibition of proteasome activity has been shown to alter the physicochemical properties of PrP (7, 8). Proteasome function is essential for normal ERAD and relief of ER stress under damage conditions. Moreover, proteasome inhibition has been shown to trigger ER stress (46, 47). To study the effect of ER stress in PrP properties and prion replication, we analyzed first the relationship between proteasome functioning and ER homeostasis. After treatment of Neuro2A cells overexpressing low levels of mouse PrP (mPrP-N2A) with two different proteasome inhibitors (epoxomycin and MG132), an increase in PrP level was observed (Fig. 1*A*). Because the three glycosylation forms of PrP

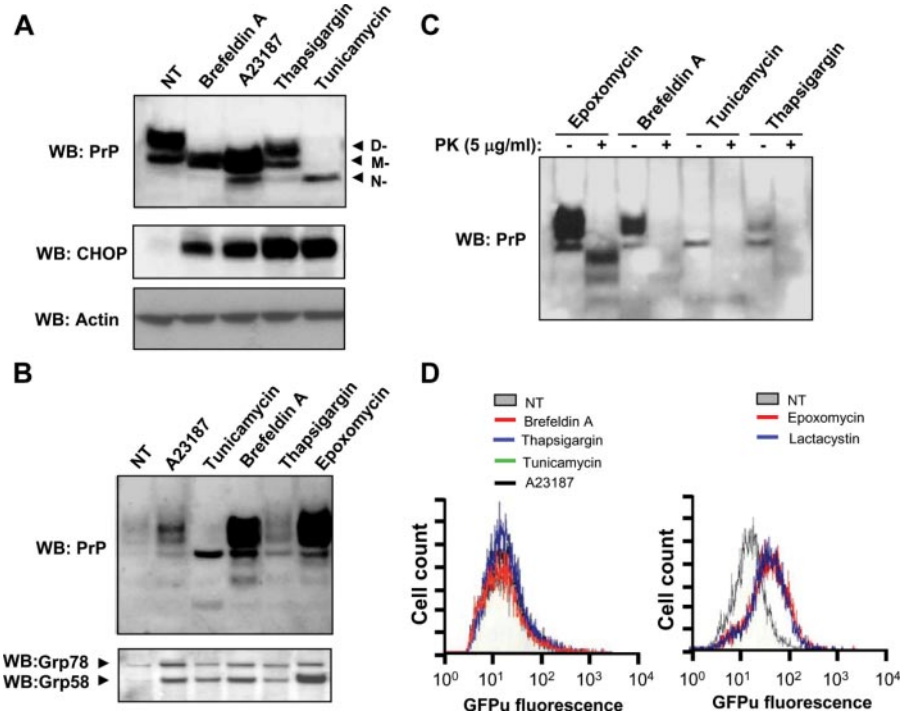

FIGURE 2. **ER stress alters the physicochemical properties of PrP independent of the proteasome.** N2A-mPrP cells were treated for 16 h with 6 μM epoxomycin, 50 μM brefeldin A, 1.3 μM A23187, 1 μg/ml tunicamycin, or 6 μM thapsigargin. *A*, in cells undergoing ER stress, total PrP, GADD153/CHOP, and actin levels were determined by Western blot. In the *upper panel*, *D-*, *M-*, and *N-* correspond to the di-, mono-, and non-glycosylated forms of PrP. *B*, in parallel, after the indicated treatments, detergent insolubility was determined in samples centrifuged in 5% Sarkosyl, and the quantity of PrP in the pellet was analyzed by Western blot. Co-precipitation of Grp58 and Grp78 in the same samples is shown. *C*, protein extracts from cells treated with ER stressors or epoxomycin were digested with 5 μg/ml PK or left untreated, and PrP levels were analyzed by Western blot. *D*, proteasome activity was monitored in cells stably expressing GFPu by fluorescence-activated cell sorting analysis. GFP fluorescence emission was determined in cells treated for 6 h with ER stress inducers (50 μM brefeldin A, 6 μM thapsigargin, 1 μg/ml tunicamycin, or 1.3 μM A23187) or proteasome inhibitors (6 μM epoxomycin or 15 μM lactacystin), and data are shown in the *right* and *left graphs*, respectively. *NT*, non-treated cells.

are all increased upon proteasome inhibition, this effect may be due in part to an increase activity of the cytomegalovirus promoter used to overexpress PrP, as previously reported (48). Analysis of several ER stress markers revealed that proteasome inhibition altered the homeostasis of the ER, reflected in the induction of the ER stress marker GADD153/CHOP, and the ER chaperones Grp58 and Grp78/BiP (Fig. 1*A*). In addition, prolonged proteasome treatment (24 h) led to activation of the ER resident caspase-12, as measured by a decrease in the levels of the inactive pro-caspase-12 form (Fig. 1*A*). It is well known that *in vitro* it is very difficult to observe the caspase-12 active fragments, and it is commonly used as a measure of the activation of this caspase, the decrease of the precursor (38). In agreement with this observation, overexpression of a dominant negative form of caspase-12 (the catalytic mutant caspase-12(C298A)) (38) decreased cellular death induced by three different proteasome inhibitors compared with cells transfected with empty vector (Fig. 1*B*). These data indicate that proteasome inhibition triggers ER stress, and this pathway mediates at least in part cellular death induced by proteasome dysfunction.

ER Stress Induces the Aggregation of PrP^C—Based on the observation that proteasome inhibition triggers ER stress, we assessed the putative contribution of ER stress *per se* to PrP misfolding. mPrP-N2A cells were treated with four different drugs known to alter the ER homeostasis, including tunicamycin (a *N*-glycosylation inhibitor), brefeldin A (an ER-Golgi trafficking inhibitor), thapsigargin (an ER-calcium ATPase inhibitor), and A23187 (a calcium ionophore). Acting through different mechanisms, all these drugs lead to ER stress and UPR activation by inducing the accumulation of misfolded proteins in the ER (20). As expected, tunicamycin led to an accumulation of the non-glycosylated form of PrP and brefeldin A treatment generated an intermediate electrophoretic pattern associated with immature glycosylation (Fig. 2*A*). Thapsigargin treatment did not alter the glycosylation of the protein, and the calcium ionophore resulted in a similar effect as brefeldin A (Fig. 2*A*). PrP expression levels after these treatments are not significantly different from untreated cells, except for the case of tunicamycin. As expected, treatment with these ER stressors led to up-regulation of GADD153/CHOP (Fig. 2*A*). All ER stressors tested induced, at different extents, the aggregation of PrP^C, as measured by the recovery of the protein in the pellet after centrifugation in non-denaturing detergents (Fig. 2*B*). As a positive control, an experiment with cells treated with the proteasome inhibitor epoxomycin resulted in the generation of extensive amounts of detergent-insoluble PrP (Fig. 2*B*), as previously described (7, 8, 18). Interestingly, co-precipitation of Grp78 and Grp58 was observed in the detergent-insoluble protein pellets containing aggregated PrP in all treatments tested when compared with control experiments (Fig. 2*B*).

The sensitivity of PrP to PK treatment was also assessed. None of the ER stress treatments tested turned PrP into a protease-resistant form even after mild protease treatment (5 μg/ml PK, Fig. 2*C*). In contrast, cells treated with epoxomycin showed PK-resistant PrP after treatment with 5 μg/ml PK. No PK-resistant PrP was observed by epoxomycin treatment after incubations with higher concentration of PK normally used to detect PrP^{Sc} from scrapie-infected brain samples (such as 50 μg/ml PK; data not shown). It is important to mention that proteasome inhibition lead to the generation of PK-resistant species with different molecular weight than PrP^{Sc} obtained from scrapie-infected mice, suggesting that their protein conformations may be different.

To study whether the effect of ER stress on PrP^C aggregation was mediated by proteasome dysfunction (an indirect effect), we analyzed the proteasome activity of living cells undergoing ER stress. To monitor proteasome activity, we stably trans-

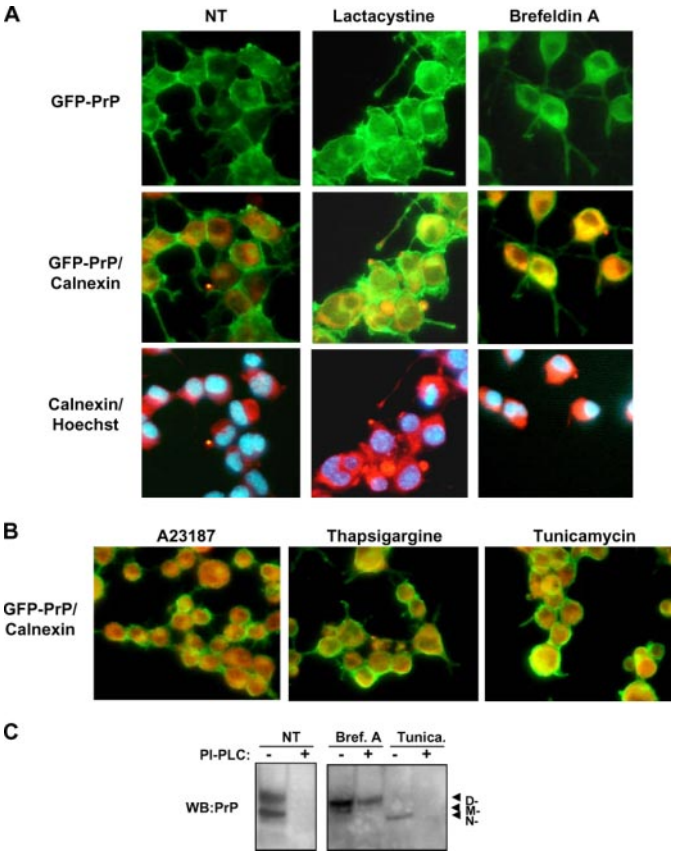

FIGURE 3. **Subcellular localization of PrP in cells undergoing ER stress.** *A*, Neuro2A cells expressing a GFP-PrP fusion protein were treated with 15 μM lactacystin or 50 μM brefeldin A, and PrP distribution was analyzed by immunofluorescence (*green fluorescence*). As intracellular markers, calnexin staining (*red fluorescence*) and nuclear staining (Hoechst, *blue*) were used. Superposition of PrP and calnexin staining resulted in a *yellow color*. *B*, merged pictures from GFP-PrP and calnexin staining is shown in cells treated with 6 μM thapsigargin, 1 μg/ml tunicamycin, or 1.3 μM A23187 for 16 h. *C*, cells treated with tunicamycin (*Tunica.*) or brefeldin A (*Bref. A*) as described in Fig. 3*B*, were treated with phosphatidylinositol-phospholipase C (*PI-PLC*) for 5 h or left untreated, and detergent-insoluble PrP was separated as described under "Materials and Methods." *NT*, non-treated cells.

fected Neuro2A cells with an expression vector for the reporter protein GFPu, a GFP fusion protein with a proteasome degradation signal (49). Fluorescence-activated cell sorting analysis of N2A-GFPu cells treated with brefeldin A, tunicamycin, A23187, or thapsigargin for 6 h revealed no alteration in the basal GFPu fluorescence, suggesting no alteration in the proteasome activity (Fig. 2*D*, *left panel*). As a positive control, cells were treated with proteasome inhibitors (epoxomycin or lactacystin), observing an accumulation of GFPu reflected in an increase in the fluorescence intensity emission (Fig. 2*D*, *right panel*). These results suggest that the generation of detergent-insoluble PrP aggregates under ER stress conditions is not associated with alteration of the proteasome activity.

Normal PrP^C Intracellular Trafficking in Cells Undergoing ER Stress—To study the influence of ER stress in PrP maturation process we stably expressed a GFP-PrP fusion protein in Neuro2A cells. As shown in Fig. 3*A*, under non-stress condition most of GFP-PrP is associated to the plasma membrane. Treatment of cells with lactacystin leads to a partial intracellular accumulation of GFP-PrP. As expected, because brefeldin A inhibits ER-Golgi trafficking, treatment with this ER stress agent resulted in intracellular accumulation of GFP-PrP (Fig. 3*A*). Remarkably, a significant fraction of the protein reached the cell surface under ER stress conditions (Fig. 3, *A* and *B*). To determine if the abnormally folded PrP molecules generated by perturbation of ER homeostasis reached the outer face of the plasma membrane, cells undergoing ER stress were treated with phosphatidylinositol-phospholipase C to eliminate the cell surface PrP by cleaving the glycosylphosphatidylinositol anchor. As shown in Fig. 3*C*, phosphatidylinositol-phospholipase C treatment decreased the amount of detergent-insoluble PrP detected in cell extracts after induction of ER stress with brefeldin A or tunicamycin. These results indicate that, under stress conditions, a fraction of PrP molecules exhibiting the abnormal properties can pass the ER quality control and appear in the plasma membrane, where Prion replication is proposed to occur (50). The interpretation of these results is that PrP insolubility is not due to an alteration in membrane interaction, but rather the form produced by ER stress likely represents a conformational intermediate with a different folding and/or aggregation characteristics than PrP^C.

ER Stress Triggers PrP^C Misfolding and Aggregation in Primary Cortical Neurons—To confirm and support our observations in an experimental system not dependent on PrP^C overexpression, we performed experiments in primary neuronal cultures from embryonic brain cortex. In agreement with the results described in Neuro2A cells, treatment of primary neuronal cultures with different ER stress agents induced to different extents the misfolding and aggregation of endogenous PrP^C (Fig. 4*A*), without changing substantially total PrP levels. No PK-resistant PrP was generated under these conditions (data not shown). Treatment induced a strong ER stress response, associated with the activation of the three main signaling branches of the UPR. Activation of IRE1α was assessed by measuring *xbp-1* mRNA splicing (Fig. 4*B*) and the expression of spliced XBP-1 protein (Fig. 4*C*). Activation of PERK signaling was determined by analyzing the expression levels of ATF4 (Fig. 4*C*) and the up-regulation of its target genes *grp78/bip* and *CHOP/GADD153* (Fig. 4*D*). ATF6 activation was indirectly detected by measuring the up-regulation of *xbp-1* mRNA levels by quantitative reverse transcription-PCR (Fig. 4*D*) (51).

Activation of the UPR Prevents PrP^C Aggregation—The UPR is a survival pathway that aims the restoration of ER homeostasis under conditions of stress. The ER stress sensors IRE1α, PERK, and ATF6 control the up-regulation of many chaperones, foldases, and proteins involved on ERAD to reduce the unfolded protein load in this organelle (20). To determine the relative contribution of each stress sensor to PrP^C misfolding under ER stress conditions, we transiently transfected different components of the UPR. As shown in Fig. 5, the co-expression of 3F4-tagged PrP with a dominant negative form of IRE1α (a carboxyl terminus deletion mutant lacking any enzymatic activity) or with a dominant negative form of its downstream target XBP-1 (43), led to a significant increase in PrP misfolding and aggregation in cells undergoing ER stress (Fig. 5*A*). In agreement with these observations, overexpression of the active form of XBP-1 (spliced XBP-1 termed XBP-1s) completely blocked PrP^C aggregation under the same conditions (Fig. 5*A*). Similarly, expression of the transcriptional factor

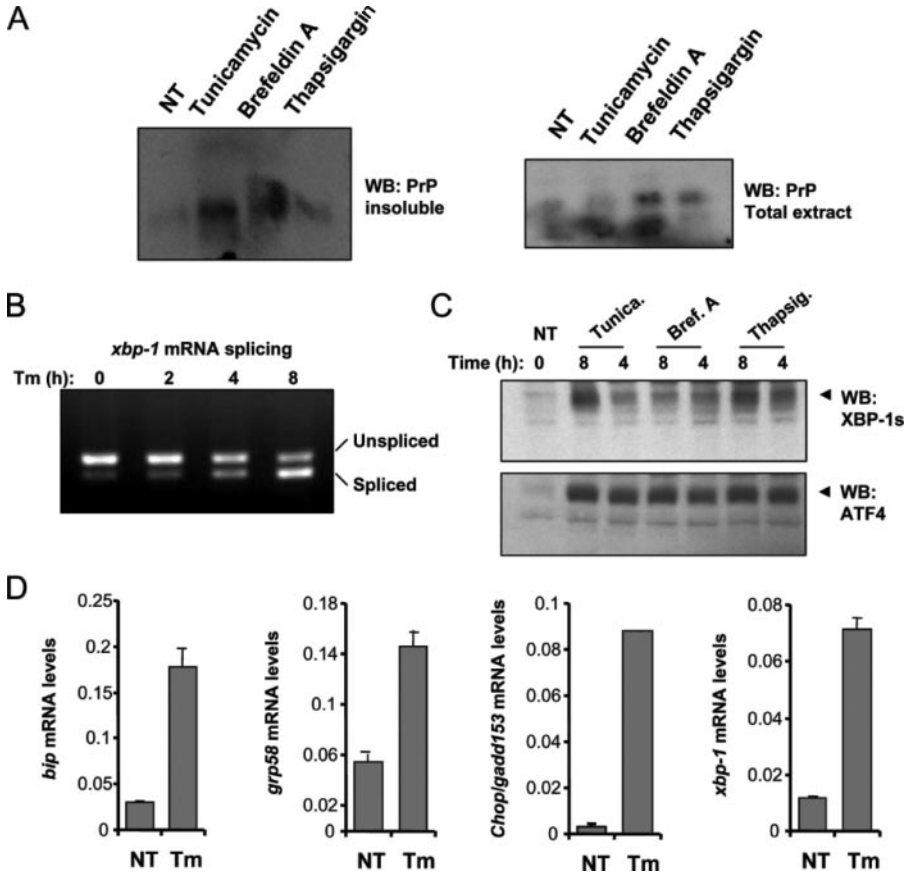

FIGURE 4. **ER stress triggers the aggregation of PrP^C in primary neuronal cultures.** *A*, primary cortical neurons from embryonic day E16.5 were treated with 10 μg/ml tunicamycin, 1 μM thapsigargin, or 20 μM brefeldin A for 16 h. The level of detergent-insoluble PrP was determined in protein extracts centrifuged in 5% Sarkosyl by measuring the quantity of PrP in the pellet by Western blot (*left blot*). Total levels of PrP are shown in the same extracts (*right blot*). *B*, primary cortical neurons were treated with 10 μg/ml tunicamycin for the indicated time points, and the splicing of *xbp-1* mRNA was determined by reverse transcription-PCR of total cDNA samples. Spliced and non-spliced XBP-1 PCR fragments are indicated. *C*, in parallel, primary neuronal cultures were treated with 10 μg/ml tunicamycin, 1 μM thapsigargin, or 20 μM brefeldin A for the indicated time points or left untreated (*NT*), and the expression levels of spliced XBP-1 protein (*XBP-1s*) and ATF4 were analyzed by Western blot. *D*, up-regulation of the mRNA for *grp78/BiP*, *grp58*, *chop/gadd153*, and *xbp-1* was quantified by real-time PCR and normalized with the levels of β-actin in cells treated with 10 μg/ml tunicamycin (*Tm*) for 8 h.

ATF4 or an active form of ATF6 (cleaved cytosolic ATF6) drastically reduced the generation of detergent-insoluble PrP^C species in cells treated with brefeldin A. Co-expression of CHOP/GADD153 with PrP^C did not affect the aggregation of PrP^C (Fig. 5*A*). No significant alterations in total PrP^C expression levels or spontaneous aggregation of PrP^C (in the absence of ER stress) were observed by overexpressing the mentioned UPR proteins (Fig. 5*A*). Thus, activation of the UPR has a protective role against PrP^C misfolding under ER stress conditions. Fig. 5*B* shows the expression levels of the UPR proteins in the cells used in these experiments.

PrP^C from ER-stressed Cells Is Highly Susceptible to Conversion to PrP^{Sc} in Vitro—We have previously described a method called protein misfolding cyclic amplification (PMCA) to induce prion replication *in vitro* (39). The PMCA technology was designed to convert a large quantity of PrP^C into PrP^{Sc} triggered by minute quantities of the misfolded protein (52). Strikingly, the *in vitro* generated PrP^{Sc} is infectious to wild-type animals producing a disease with identical characteristics as the infectious agent isolated from brains of sick animals (53). Several pieces of evidence suggest that prion replication involves the formation of a conformational intermediate produced by interaction of PrP^C with a host-encoded conversion factor (41, 54, 55). The biochemical differences in the PrP form produced upon ER stress led us to hypothesize that this PrP conformer may represent such an intermediate. We tested this hypothesis by using extracts from cells subjected to ER stress as a substrate for PMCA. For these studies we used Neuro2A cells overexpressing mouse PrP with the 3F4 epitope (N2A-PrP3F4). This allowed us to unmistakably differentiate newly generated PrP^{Sc} from the one present in the scrapie-brain inoculum used as a seed for PMCA (Fig. 6*A*). N2A-PrP3F4 cells were left untreated or stimulated with 50 μM brefeldin A or 6 μM epoxomycin for 16 h to induce ER stress. Post-nuclear extracts containing similar quantities of PrP were subjected to PMCA using two different dilutions of Rocky Mountain Laboratory-scrapie brain homogenates as the source of PrP^{Sc}. As expected, no PK-resistant PrP^{Sc} from PrP-3F4 was observed in the mixture before PMCA. Interestingly, in cell extracts from brefeldin A- or epoxomycin-treated cells, higher levels of PrP^{Sc} were produced after PMCA compared with an experiment made with extracts from non-treated cells (Fig. 6*B*). The conversion rate using ER-stressed cells was several-fold higher than that obtained with untreated cells, and these differences were not due to distinct quantities of PrP^C, because the same levels of PrP were used in all experiments (Fig. 6*B*, *right panel*). We also attempted to assess the effect of ER stress on prion replication in living cells, using Neuro2A cells chronically infected with Rocky Mountain Laboratory-scrapie prions. However, these experiments were not possible, because ER stressors are cytotoxic after prolonged treatments (data not shown).

DISCUSSION

Growing evidence indicates that the ER plays a role not only in PrP synthesis and maturation, but also is intimately implicated in PrP toxicity and in the formation of the disease-associated misfolded protein (reviewed in Ref. 5). Expression of several mutant PrP molecules associated with human hereditary TSEs resulted in the formation of cytotoxic PrP forms that were retained early in the secretory pathway (9, 16, 55, 56). Stimula-

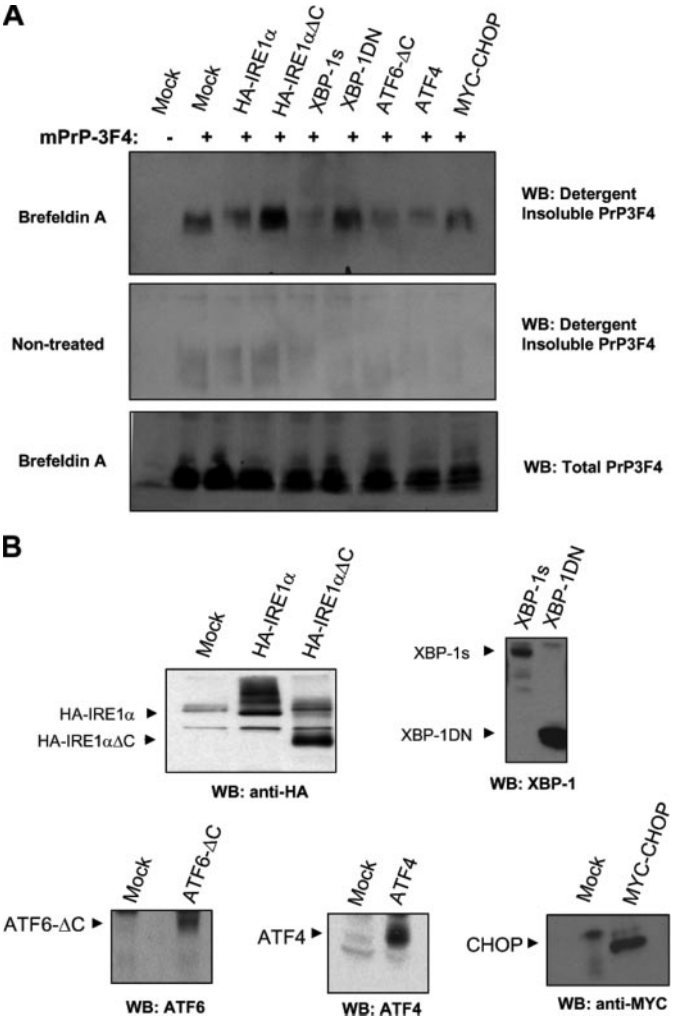

FIGURE 5. **Activation of the UPR decreases PrP^C aggregation under ER stress conditions.** *A*, Neuro2A cells were transiently co-transfected with an expression vector for mPrP-3F4 in the presence or absence of expression vectors for HA-IRE1α, HA-IRE1αΔC (dominant negative form of IRE1α), XBP-1 active form (XBP-1s, spliced XBP-1), dominant negative XBP-1 (XBP-1DN), active ATF6 (ATF6ΔC), ATF4, MYC-CHOP, or empty pDNA.3 vector (mock). Forty-eight hours after the transfection, cells were treated with 10 μM brefeldin A for 16 h or left untreated, and the generation of detergent-insoluble PrP-3F4 species was analyzed by Western blot. All results are representative of three independent experiments. *B*, control experiments to assess the expression levels by Western blot analysis of HA-IRE1α, HA-IRE1αΔC, XBP-1s, XBP-1DN, ATF6ΔC, ATF4, and MYC-CHOP in the experiments described in *A*.

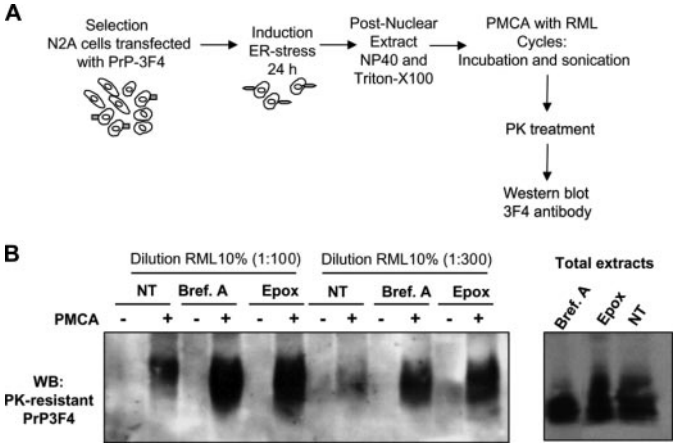

FIGURE 6. **ER stress facilitates prion replication.** *A*, schematic representation of the experimental procedure used to study the influence of ER stress on prion replication. *B*, Neuro2A cells stably expressing mPrP-3F4 were treated with 50 μM brefeldin A (*Bref. A*) or 6 μM epoxomycin (*Epox*) for 16 h, and post-nuclear cell lysates were mixed with Rocky Mountain Laboratory scrapie brain homogenate (at 1:100 or 1:300 dilution) and subjected to eight cycles of incubation and sonication (PMCA). The formation of protease-resistance PrP^{Sc} was analyzed by Western blot after treatment of extracts with 50 μg/ml of PK as described under "Materials and Methods." The levels of PrP-3F4 in the total extracts before PK treatment are shown in the *right panel*.

tion of retrograde transport toward the ER increases the accumulation of PrP^{Sc} in prion-infected neuroblastoma cells (57). Scrapie infection triggers changes on PrP^C glycosylation suggesting that the homeostasis of the ER and Golgi is altered by prion replication (58, 59). Finally, alteration of ER function is involved in the neuronal death process observed in infectious forms of TSEs (32, 37, 38).

It has been proposed that proteasomal dysfunction may participate in PrP^{Sc}-induced neurodegeneration by producing the general accumulation of abnormally folded and immature proteins in the ER (6). This protein "traffic jam" may activate cell death pathways involved in the ER stress response. Our results support the notion that the mechanism by which proteasome dysfunction induces cellular death is through the induction of ER stress, as measured by an increased expression of GADD153/CHOP, ER chaperones, and caspase-12 processing. These data led us to study the possibility that ER stress may promote the generation of PrP^{Sc}-like species. Our results showed that treatment of Neuro2A cells with compounds that alter ER homeostasis generated a PrP isoform that was detergent-insoluble but not protease-resistant. Similar observations were obtained with primary neuronal cultures treated with ER stress agents. Immunolocalization experiments revealed that a significant fraction of this misfolded PrP isoform reached the plasma membrane, indicating that ER stress changes the folding of the protein rather than its membrane association. Conversely, inhibition of proteasome activity with epoxomycin resulted in a different form of PrP, which is both insoluble and mildly PK-resistant, confirming previous reports (7). The effect of ER stress on PrP properties was not mediated by modification of the proteasome, as measured by the expression of GFPu, a marker used to monitor proteasome activity.

The differences observed between the effects of ER stress and proteasome inhibition suggest a different mechanism triggering PrP misfolding. Proteasome inhibitors produce accumulation of abnormal PrP molecules subjected to ERAD in addition to altering ER homeostasis. In the case of PrP misfolding generated under ER stress, a general alteration of the ER-folding machinery may trigger an extensive modification of the PrP folding pathway. Consequences of ER stress include differential expression of chaperones in the ER, changes in the environmental properties of this organelle, or alteration of the protein quality control. In agreement with this hypothesis, manipulation of UPR signaling by overexpressing different components of the pathway, such as the transcriptional factors XBP-1, ATF4, and ATF6, significantly reduced PrP^C aggregation under ER stress conditions. Conversely, expression of a dominant negative form of IRE1α or XBP-1 increased the aggregation of PrP^C under similar conditions. These findings indicate that UPR activation reduces PrP misfolding. In agreement with our

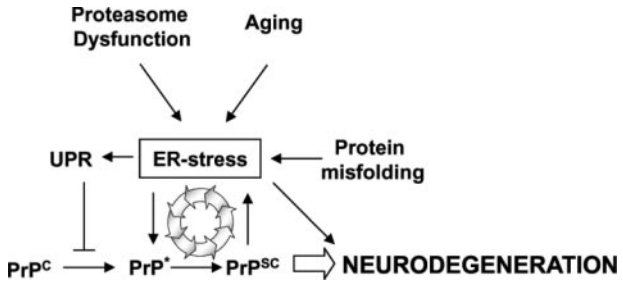

FIGURE 7. **Schematic model for the relationship between alterations in ER homeostasis, PrP misfolding, and neurodegeneration.** Our findings suggest that ER stress may play a central role in prion replication and neurodegeneration associated with TSEs. The data points to a vicious cycle in which PrP^{Sc} formation promotes ER stress, which in turn facilitates prion replication by inducing the partial misfolding and aggregation of PrP^{C} (denoted as *PrP**). Activation of the UPR by ER stress conditions may have a protective effect by preventing the misfolding of PrP.

findings, a recent report described the accumulation of small quantities of misfolded PrP species in the cytosol in cells treated with ER stressors, due to a decreased translocation of PrP into the ER (36). Overexpression of spliced XBP-1 protein prevented this process, indicating that the UPR may also control the targeting of PrP to the ER. In a related study done in yeast cells, expression of PrP led to generation of misfolded PrP molecules that are degraded by ERAD (35). More importantly, overexpression of PrP leads to growth impairment in yeast cells deficient in IRE1 (35), the only ER stress sensor present in yeast. Taken together, these data suggest that the UPR has an active role in controlling PrP pathogenesis. We are currently evaluating the contribution of ER stress on prion pathogenesis *in vivo* by infecting with scrapie prions mice genetically deficient in different UPR components.

It has been hypothesized that the prion conversion process involves the generation of a folding intermediate, termed PrP*, which likely represents a partially unfolded form of PrP^{C} with exposed fragments to permit the interaction with PrP^{Sc} (1, 41, 55). In the cell it is thought that PrP* is formed upon interaction of PrP^{C} with an as yet unidentified conversion factor (1, 41). The changes of the biochemical properties of wild-type PrP^{C} observed in the current study prompted us to investigate if the misfolded PrP molecule produced upon ER-stress may represent a PrP*-like form. Analysis of PrP^{Sc} generation *in vitro* using PMCA (39) showed that PrP substrates derived from cells treated with ER stress-inducing drugs or proteasome inhibitors increased the rate of prion replication (Fig. 6*B*). The infectious properties of this *in vitro* generated PrP^{Sc} remains to be determined, but its biochemical properties are identical to those observed with PrP^{Sc} generated from control cells. We cannot rule out that activation of ER stress may alter the expression of chaperones and folding enzymes that could influence the efficiency of prion structural conversion by PMCA.

We propose that ER stress leads to the accumulation of a PrP substrate that is more prone to be converted into PrP^{Sc}, which may facilitate prion replication under disease conditions (Fig. 7). Imbalances of ER homeostasis are a frequent event in aging (60), which may provide a molecular explanation for the fact that most forms of TSE appear in elderly people. In addition, considering previous reports from our group and other groups showing that PrP^{Sc} replication induces ER stress, our current findings point to the existence of a vicious cycle, in which the induction of ER stress by prion infection may promote conformational changes in PrP^{C} rendering the protein more susceptible to be converted into PrP^{Sc}. These cycles may result in an amplification loop leading to an exponential increase in PrP^{Sc} generation, neuronal dysfunction, and disease (Fig. 7). Therefore, ER stress seems to play a central and crucial role in the development of prion diseases. In addition, there is growing evidence suggesting that ER stress and the UPR is involved in other protein conformational disorders (for a review, see Refs. 20), such as Parkinson disease (47, 61, 62), amyotrophic lateral sclerosis (63–67), Huntington disease (68, 69), and Alzheimer disease (70). Our findings provide an alternative therapeutic target for intervention against prion diseases. Compounds protecting ER homeostasis such as chemical chaperons (71, 72) or disrupting the connection between alterations in ER functioning and PrP misfolding may be able to delay substantially prion replication and disease onset.

Acknowledgments—We thank Dr. Walker Jackson, Kinsey Maundrell, and Milene Russelakis-Carneiro for helpful discussions about this work. We also thank Dr. R. Rao (Buck Institute for Age Research) for kindly providing the caspase-12 dominant-negative mutant, Laurie Glimcher (Harvard School of Public Health) for providing expression vectors for XBP-1, ATF6, and anti-XBP-1 antibody, David Ron (New York University) for providing expression vectors for ATF4 and CHOP, and R. Kopito (Stanford University) for providing us the GFPu expression vector.

REFERENCES

1. Prusiner, S. B. (1998) *Proc. Natl. Acad. Sci. U. S. A.* **95,** 13363–13383
2. Hegde, R. S., and Rane, N. S. (2003) *Trends Neurosci.* **26,** 337–339
3. Harris, D. A. (2003) *Br. Med. Bull.* **66,** 71–85
4. Vey, M., Pilkuhn, S., Wille, H., Nixon, R., DeArmond, S. J., Smart, E. J., Anderson, R. G., Taraboulos, A., and Prusiner, S. B. (1996) *Proc. Natl. Acad. Sci. U. S. A.* **93,** 14945–14949
5. Hetz, C. A., and Soto, C. (2006) *Curr. Mol. Med.* **6,** 37–43
6. Dimcheff, D. E., Portis, J. L., and Caughey, B. (2003) *Trends Cell Biol.* **13,** 337–340
7. Ma, J., and Lindquist, S. (2001) *Proc. Natl. Acad. Sci. U. S. A.* **98,** 14955–14960
8. Yedidia, Y., Horonchik, L., Tzaban, S., Yanai, A., and Taraboulos, A. (2001) *EMBO J.* **20,** 5383–5391
9. Jin, T., Gu, Y., Zanusso, G., Sy, M., Kumar, A., Cohen, M., Gambetti, P., and Singh, N. (2000) *J. Biol. Chem.* **275,** 38699–38704
10. Zanusso, G., Petersen, R. B., Jin, T., Jing, Y., Kanoush, R., Ferrari, S., Gambetti, P., and Singh, N. (1999) *J. Biol. Chem.* **274,** 23396–23404
11. Singh, N., Zanusso, G., Chen, S. G., Fujioka, H., Richardson, S., Gambetti, P., and Petersen, R. B. (1997) *J. Biol. Chem.* **272,** 28461–28470
12. Gu, Y., Verghese, S., Mishra, R. S., Xu, X., Shi, Y., and Singh, N. (2003) *J. Neurochem.* **84,** 10–22
13. Drisaldi, B., Stewart, R. S., Adles, C., Stewart, L. R., Quaglio, E., Biasini, E., Fioriti, L., Chiesa, R., and Harris, D. A. (2003) *J. Biol. Chem.* **278,** 21732–21743
14. Stewart, R. S., Drisaldi, B., and Harris, D. A. (2001) *Mol. Biol. Cell* **12,** 881–889
15. Ivanova, L., Barmada, S., Kummer, T., and Harris, D. A. (2001) *J. Biol. Chem.* **276,** 42409–42421
16. Campana, V., Sarnataro, D., Fasano, C., Casanova, P., Paladino, S., and Zurzolo, C. (2006) *J. Cell Sci.* **119,** 433–442
17. Ma, J., and Lindquist, S. (2002) *Science* **298,** 1785–1788
18. Ma, J., Wollmann, R., and Lindquist, S. (2002) *Science* **298,** 1781–1785

19. Kristiansen, M., Messenger, M. J., Klohn, P. C., Brandner, S., Wadsworth, J. D., Collinge, J., and Tabrizi, S. J. (2005) *J. Biol. Chem.* **280,** 38851–38861
20. Schroder, M., and Kaufman, R. J. (2005) *Annu. Rev. Biochem.* **74,** 739–789
21. Hetz, C. A., and Soto, C. (2006) *Curr. Mol. Med.* **6,** 1
22. Calfon, M., Zeng, H., Urano, F., Till, J. H., Hubbard, S. R., Harding, H. P., Clark, S. G., and Ron, D. (2002) *Nature* **415,** 92–96
23. Lee, K., Tirasophon, W., Shen, X., Michalak, M., Prywes, R., Okada, T., Yoshida, H., Mori, K., and Kaufman, R. J. (2002) *Genes Dev.* **16,** 452–466
24. Lee, A. H., Iwakoshi, N. N., and Glimcher, L. H. (2003) *Mol. Cell Biol.* **23,** 7448–7459
25. Haze, K., Yoshida, H., Yanagi, H., Yura, T., and Mori, K. (1999) *Mol. Biol. Cell* **10,** 3787–3799
26. Marciniak, S. J., Yun, C. Y., Oyadomari, S., Novoa, I., Zhang, Y., Jungreis, R., Nagata, K., Harding, H. P., and Ron, D. (2004) *Genes Dev.* **18,** 3066–3077
27. Zinszner, H., Kuroda, M., Wang, X., Batchvarova, N., Lightfoot, R. T., Remotti, H., Stevens, J. L., and Ron, D. (1998) *Genes Dev.* **12,** 982–995
28. Oakes, S. A., Lin, S. S., and Bassik, M. C. (2006) *Curr. Mol. Med.* **6,** 99–109
29. Nakagawa, T., Zhu, H., Morishima, N., Li, E., Xu, J., Yankner, B. A., and Yuan, J. (2000) *Nature* **403,** 98–103
30. Yoneda, T., Imaizumi, K., Oono, K., Yui, D., Gomi, F., Katayama, T., and Tohyama, M. (2001) *J. Biol. Chem.* **276,** 13935–13940
31. Rao, R. V., Castro-Obregon, S., Frankowski, H., Schuler, M., Stoka, V., del Rio, G., Bredesen, D. E., and Ellerby, H. M. (2002) *J. Biol. Chem.* **277,** 21836–21842
32. Brown, A. R., Rebus, S., McKimmie, C. S., Robertson, K., Williams, A., and Fazakerley, J. K. (2005) *Biochem. Biophys. Res. Commun.* **334,** 86–95
33. Yoo, B. C., Krapfenbauer, K., Cairns, N., Belay, G., Bajo, M., and Lubec, G. (2002) *Neurosci. Lett.* **334,** 196–200
34. Ferreiro, E., Resende, R., Costa, R., Oliveira, C. R., and Pereira, C. M. (2006) *Neurobiol. Dis.* **23,** 669–678
35. Apodaca, J., Kim, I., and Rao, H. (2006) *Biochem. Biophys. Res. Commun.* **347,** 319–326
36. Orsi, A., Fioriti, L., Chiesa, R., and Sitia, R. (2006) *J. Biol. Chem.* **281,** 30431–30438
37. Hetz, C., Russelakis-Carneiro, M., Walchli, S., Carboni, S., Vial-Knecht, E., Maundrell, K., Castilla, J., and Soto, C. (2005) *J. Neurosci.* **25,** 2793–2802
38. Hetz, C., Russelakis-Carneiro, M., Maundrell, K., Castilla, J., and Soto, C. (2003) *EMBO J.* **22,** 5435–5445
39. Saborio, G. P., Permanne, B., and Soto, C. (2001) *Nature* **411,** 810–813
40. Bence, N. F., Bennett, E. J., and Kopito, R. R. (2005) *Methods Enzymol.* **399,** 481–490
41. Saborio, G. P., Soto, C., Kascsak, R. J., Levy, E., Kascsak, R., Harris, D. A., and Frangione, B. (1999) *Biochem. Biophys. Res. Commun.* **258,** 470–475
42. Hetz, C., Bernasconi, P., Fisher, J., Lee, A. H., Bassik, M. C., Antonsson, B., Brandt, G. S., Iwakoshi, N. N., Schinzel, A., Glimcher, L. H., and Korsmeyer, S. J. (2006) *Science* **312,** 572–576
43. Lee, A. H., Iwakoshi, N. N., Anderson, K. C., and Glimcher, L. H. (2003) *Proc. Natl. Acad. Sci. U. S. A.* **100,** 9946–9951
44. Lee, A. H., Chu, G. C., Iwakoshi, N. N., and Glimcher, L. H. (2005) *EMBO J.* **24,** 4368–4380
45. Iwakoshi, N. N., Lee, A. H., Vallabhajosyula, P., Otipoby, K. L., Rajewsky, K., and Glimcher, L. H. (2003) *Nat. Immunol.* **4,** 321–329
46. Jiang, H. Y., and Wek, R. C. (2005) *J. Biol. Chem.* **280,** 14189–14202
47. Tsai, Y. C., Fishman, P. S., Thakor, N. V., and Oyler, G. A. (2003) *J. Biol. Chem.* **278,** 22044–22055
48. Roucou, X., Guo, Q., Zhang, Y., Goodyer, C. G., and LeBlanc, A. C. (2003) *J. Biol. Chem.* **278,** 40877–40881
49. Bence, N. F., Sampat, R. M., and Kopito, R. R. (2001) *Science* **292,** 1552–1555
50. Hetz, C., Maundrell, K., and Soto, C. (2003) *Trends Mol. Med.* **9,** 237–243
51. Yoshida, H., Matsui, T., Yamamoto, A., Okada, T., and Mori, K. (2001) *Cell* **107,** 881–891
52. Soto, C. (2002) *Biochem. Soc. Trans.* **30,** 569–574
53. Castilla, J., Saa, P., Hetz, C., and Soto, C. (2005) *Cell* **121,** 195–206
54. Cohen, F. E., and Prusiner, S. B. (1998) *Annu. Rev. Biochem.* **67,** 793–819
55. Daude, N., Lehmann, S., and Harris, D. A. (1997) *J. Biol. Chem.* **272,** 11604–11612
56. Stewart, L. R., White, A. R., Jobling, M. F., Needham, B. E., Maher, F., Thyer, J., Beyreuther, K., Masters, C. L., Collins, S. J., and Cappai, R. (2001) *J. Neurosci. Res.* **65,** 565–572
57. Beranger, F., Mange, A., Goud, B., and Lehmann, S. (2002) *J. Biol. Chem.* **277,** 38972–38977
58. Russelakis-Carneiro, M., Saborio, G. P., Anderes, L., and Soto, C. (2002) *J. Biol. Chem.* **277,** 36872–36877
59. Russelakis-Carneiro, M., Hetz, C., Maundrell, K., and Soto, C. (2004) *Am. J. Pathol.* **165,** 1839–1848
60. Rao, R. V., and Bredesen, D. E. (2004) *Curr. Opin. Cell Biol.* **16,** 653–662
61. Ryu, E. J., Harding, H. P., Angelastro, J. M., Vitolo, O. V., Ron, D., and Greene, L. A. (2002) *J. Neurosci.* **22,** 10690–10698
62. Holtz, W. A., and O'Malley, K. L. (2003) *J. Biol. Chem.* **278,** 19367–19377
63. Turner, B. J., and Atkin, J. D. (2006) *Curr. Mol. Med.* **6,** 79–86
64. Vlug, A. S., Teuling, E., Haasdijk, E. D., French, P., Hoogenraad, C. C., and Jaarsma, D. (2005) *Eur. J. Neurosci.* **22,** 1881–1894
65. Wootz, H., Hansson, I., Korhonen, L., Napankangas, U., and Lindholm, D. (2004) *Biochem. Biophys. Res. Commun.* **322,** 281–286
66. Tobisawa, S., Hozumi, Y., Arawaka, S., Koyama, S., Wada, M., Nagai, M., Aoki, M., Itoyama, Y., Goto, K., and Kato, T. (2003) *Biochem. Biophys. Res. Commun.* **303,** 496–503
67. Kikuchi, H., Almer, G., Yamashita, S., Guegan, C., Nagai, M., Xu, Z., Sosunov, A. A., McKhann, G. M., and Przedborski, S. (2006) *Proc. Natl. Acad. Sci. U. S. A.* **103,** 6025–6030
68. Nishitoh, H., Matsuzawa, A., Tobiume, K., Saegusa, K., Takeda, K., Inoue, K., Hori, S., Kakizuka, A., and Ichijo, H. (2002) *Genes Dev.* **16,** 1345–1355
69. Sekine, Y., Takeda, K., and Ichijo, H. (2006) *Curr. Mol. Med.* **6,** 87–97
70. Lindholm, D., Wootz, H., and Korhonen, L. (2006) *Cell Death Differ.* **13,** 385–392
71. Tatzelt, J., Prusiner, S. B., and Welch, W. J. (1996) *EMBO J.* **15,** 6363–6373
72. Ozcan, U., Yilmaz, E., Ozcan, L., Furuhashi, M., Vaillancourt, E., Smith, R. O., Gorgun, C. Z., and Hotamisligil, G. S. (2006) *Science* **313,** 1137–1140